On the Accumulation of Genomic Barriers to Gene Flow in the Origin of Animal Species

Derek D. Eddo, Bailey M. L. Rouse, Silu Wang*

Department of Biological Sciences
State University of New York, Buffalo

*Corresponding author email: siluwang.biodiv@gmail.com

Abstract

The accumulation of genomic barriers to gene flow underpins speciation. We synthesized decades of micro- and macroevolutionary investigations on speciation and formulated a statistical foundation to test alternative speciation genetic hypotheses: (1) the Beanbag Effect Model predicts a linear establishment of barriers to gene flow with the genetic divergence between the parental lineages; (2) the Snowball Effect Model predicts exponential spread of barriers, whereas (3) the Slowdown Effect Model predicts a logarithmic buildup of barriers. Testing the three models requires quantifying the progression of reproductive isolation as speciation unfolds in the face of gene flow. Here, we established a global hybrid zone database, Hybrid Zone Explorer, with all the animal hybrid zones reported to date. This database empowered a rare opportunity to directly infer in situ speciation with gene flow and test the three speciation rate models. We used cline width over dispersal rate, or the selection against hybrids in the tension zone model, to reflect the establishment of barriers to gene flow. The Snowball Effect Model (2) is best supported with the full dataset, implying predominant epistasis among barriers to gene flow. We further refined the three models to consider independent and interactive effects of mitochondrial (mtDNA) and nuclear genetic (nDNA) divergence on the selection against hybrids. The Snowball Effect Model (2) was again best supported by the data, revealing positive roles of independent mitonuclear genetic divergence. However, the interaction between mtDNA and nDNA divergence negatively contributed to barriers to gene flow, indicating introgressive mitonuclear discordance. Collectively, this data synthesis across animal speciation continuum is consistent with an accelerated growth of barriers to gene flow with mitonuclear genetic divergence. This speciation momentum profoundly illuminates the genomic principle shaping speciation rate heterogeneity underlying animal biodiversity on our planet.

Keywords: Speciation rate, Hybrid zone, Snowball Effect, Genetic Incompatibility, Speciation, Hybridization, Cline.

Introduction

The evolution of reproductive isolation is underpin by genetic incompatibilities, which accrue as the diverging lineages accumulate lineage-specific substitutions (Dobzhansky 1934; Mayr 1959 & 1963; Orr 1995). The increased genetic incompatibilities contribute to the selection against hybrids (Palopoli and Wu 1994; Orr 1995; Welch 2004), which attenuate gene flow between diverging lineages, allowing speciation to unfold (Gavrilets 2004; Nosil 2008; Westram et al. 2022). The rate at which lineage-specific substitutions drive the selection against hybrids ultimately prescribes the speciation rate (Coyne and Orr 1989).

The debates over this relationship have inspired decades of investigation of genomic architecture and mechanisms of speciation (Mayr 1959 & 1963; Feder et al. 2014; Nosil and Schluter 2011; Seehausen et al. 2014;). If divergent substitutions independently contribute to speciation in the face of gene flow as a 'Beanbag' genetic process (Fisher, 1941; Haldane 1964), the genetic distance between the diverging lineages should predict linear growth of genetic barriers to gene flow. However, this 'Beanbag Genetic Model' was coined and criticized by Mayr (1959) as being oversimplified for omitting epistatic effects among co-adaptive genes. If two-loci epistatic incompatibilities, or Dobzhansky & Muller Incompatibilities (DMIs) (Dobzhansky 1934; Muller 1942; Mayr 1963), predominate barriers to gene flow, the selection against hybrids would increase exponentially as genetic distance increases, reflecting a 'Snowball Effect' (Orr 1995). A greater acceleration in speciation rate would be observed if the genetic distance results in abundant higher-order incompatibilities (Orr 1995). In contrast, an early 'slowdown' might be observed if premating isolation is established prior to substantial genetic incompatibilities (Gourbiere and Mallet 2010).

Several taxon-specific empirical studies have supported the Snowball Effect hypothesis, where the increase of genetic distance between parental lineages exponentially suppresses hybrid fitness (Presgraves 2002; Matute et al. 2010; Moyle and Nakazato 2010). This simple probability model derived exponential growth of hybrid fitness reduction (S) incurred by $\binom{K}{2}$ DMIs, where K is the total number of divergent substitutions (Fig. 1). However, others reported a more gradual, linear accumulation of S in response to genetic divergence (Lijtmaer et al. 2003; Gourbiere and Mallet 2010; Stelkens et al. 2010) (Fig. 1). The linear relationship between S and K is consistent with a Beanbag Effect with additive accumulation of independent barriers to gene flow. A logarithmic relationship was also observed, reflecting a Slowdown Effect (Gourbiere and Mallet 2010), implying a diminishing return of K in the growth of S (Fig. 1). A Slowdown Effect suggests greater relative effect size of earlier established barriers to gene flow. Collectively, the taxon-specific investigations showed conflicting patterns that stimulate large-scale comparative studies to identify evolutionary regularities in speciation rates across the tree of life.

The heterogeneous patterns of speciation rate are likely attributed to the variability of locus-specific effect sizes and the probability of incompatibility in different parts of the genome. For instance, the smaller effective population size in the mitochondrial genome than the nuclear genome predicted greater drift, counteracting selection (Slatkin and Maruyama 1975). In addition, mitochondrial deleterious mutations reportedly exhibit a greater average effect size than nuclear mutations (Popadin et al. 2013). Moreover, the probability of incompatibility can differ between intergenomic and intragenomic discordance.

More broadly, the heterogeneous patterns of selection against hybrids could also be explained by the stages of speciation along the speciation continuum (Roux et al. 2016). In the early stages of divergence, large-effect single-locus genetic barriers are more effective than DMIs to overcome extensive gene flow (Felsenstein 1981; Wu 2001; Nosil and Schluter 2011; Wang et al. 2020; de Zwaan et al. 2022). If the effect sizes of single-locus barriers were constant through speciation progression, the selection against hybrids should linearly increase as lineage-specific substitutions accumulate over time (Fig. 1, Beanbag Effect). If the effect sizes were larger earlier as represented in Fisher's Geometric Model of Adaptation (Fisher 1930), when the lineage-specific substitutions were scarce and exhibiting diminishing returns in response to further increments of genetic divergence, a Slowdown Effect in the form of a logarithmic function is expected (Gourbiere and Mallet 2010) (Fig. 1, Slowdown Effect). As the gene flow between diverging lineages attenuates, allowing DMIs to build up, a Snowball Effect can be observed (Orr 1995) (Fig. 1, Snowball Effect), where the selection against hybrids grows exponentially as lineage-specific substitutions accrue. The heterogeneous tension between genetic incompatibility and gene flow across the speciation continuum is naturally encapsulated in decades of hybrid zone studies (Fig. 2).

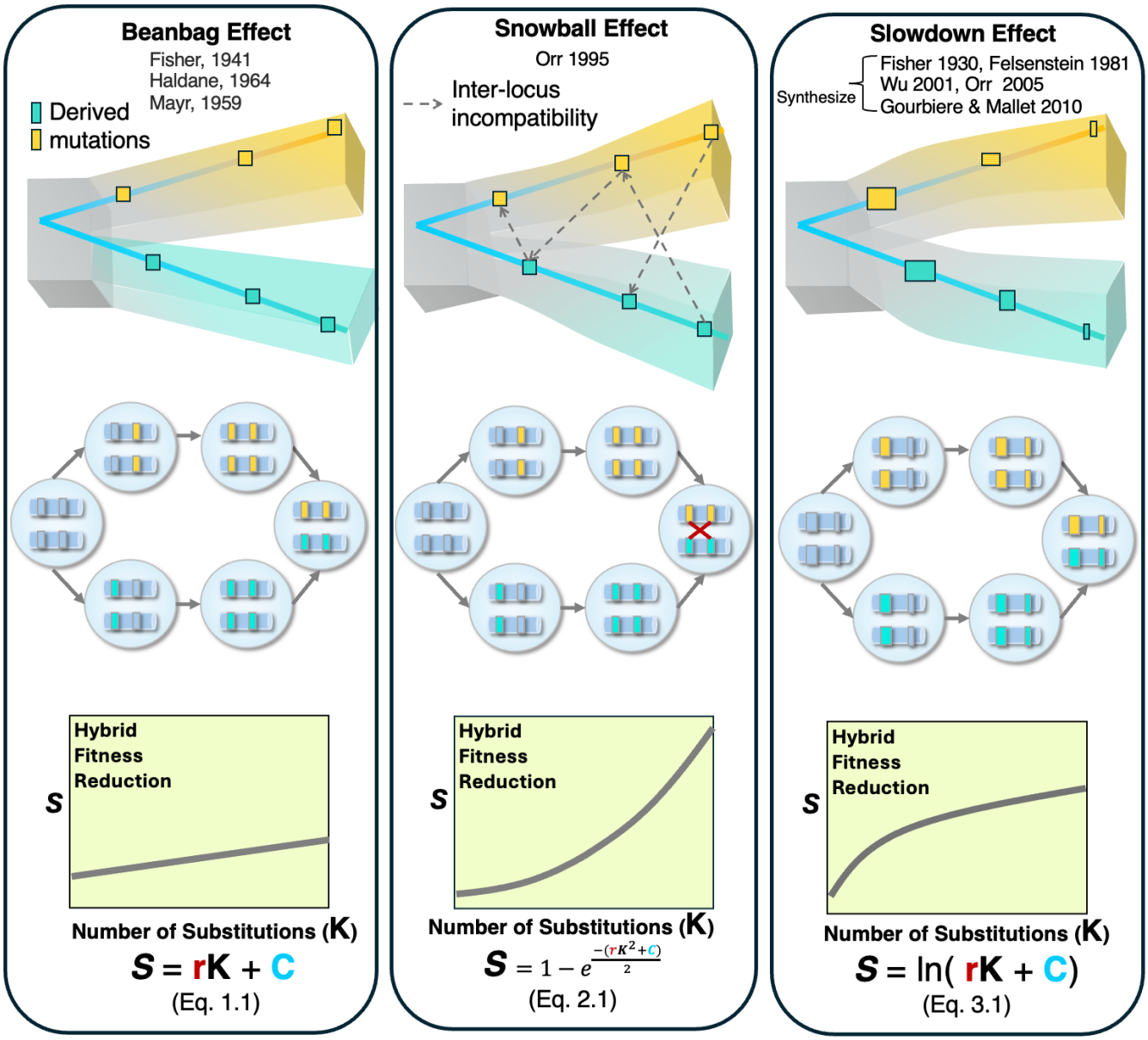


Fig. 1 Three speciation models: (1) Beanbag Effect, **(2)** Snowball Effect, and **(3)** Slowdown Effect. All three model concerns the hybrid fitness reduction (**S**) in response to the growth of the number of divergent substitutions (K) between the lineages. Snowball Effect (Orr 1995) modeled hybrid fitness reduction with $\binom{K}{2}$ pairs of incompatibilities with an average effect size *r*, thus S grows exponentially with the increase of K. Under Beanbag Effect (Fisher 1941; Haldane, 1964; Mayr, 1959) without epistasis and even fitness effects, *S* grows linearly with K. The Slowdown Effect synthesized Fisher's Geometric Model (Fisher 1930) and barriers to gene flow (Felsenstein, 1981; Wu 2001; Orr 2005), where barriers of greater effect sizes are more likely to establish when divergent substitutions are scarce.

Hybrid zones are geographic areas where diverging lineages hybridize (Barton 1979). They provide unique opportunities to observe the progression of speciation as the tension between genetic incompatibility and gene flow is resolved (Barton and Hewitt 1985). This tension is effectively theorized as the tension zone model, where the width of the cline (w) is a balance of selection (s) and dispersal (σ) (Fig. 2A) (Barton 1979). The selection coefficient (s) is a transformed ratio between cline width and dispersal rate, a composite expression of genetic incompatibility and divergent selection balancing dispersal, the emergence of reproductive isolation, or the speciation progress in the face of gene flow. The rate at which s increases with the extension of genetic distance between diverging lineages ultimately translates to the in-situ speciation rate (Fig. 2B).

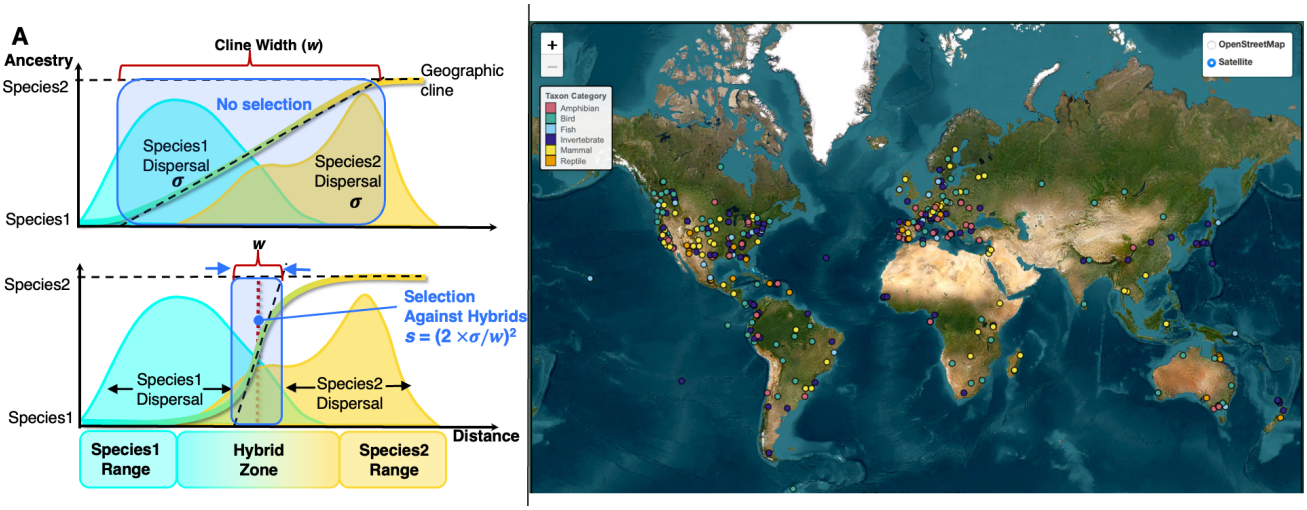


Fig.2 Hybrid zones are natural laboratories for understanding speciation. A, Illustration of the hybrid zones with (bottom) or without (top) selection. The cline width (*w*) of a hybrid zone is a balance of gene flow (***σ***) and selection (*s*) against hybrids. In the absence of *s*, ***σ*** will widen *w* over time as species 1 hybridizes with species 2 (top). Bottom: strong selection against hybrids counteracts with ***σ*** and shrinks *w*. **B**, World distribution of animal hybrid zones represented in the Hybrid Zone Explorer database. Over 315 animal hybrid zones have been reported. Color categories correspond to six different organismal groups: mammals in yellow (59), birds in green (69), reptiles in orange (25), amphibians in maroon (45), invertebrates in purple (94), and fish in blue (23).

Here, we conduct a data synthesis to examine the buildup rate of selection against hybrids (*s*) in animal hybrid zones (Fig. 2). We tested three alternative models that predict the selection against hybrids with the genetic distance between parental lineages. Model 1 predicts a linear increase of *s* as genetic distance increases (Fig. 1, Beanbag Effect); Model 2 predicts an exponential growth of *s* (Fig. 1, Snowball Effect); while Model 3 predicts a logarithmic relationship (Fig. 1, Slowdown Effect).

We further developed three refined models to dissect mitochondrial and nuclear genetic effects on speciation. Since the mitochondrial and nuclear genomes have distinct substitution rates (Ballard and Whitlock 2003) and coevolve to maintain critical eukaryotic energetics (Eddo et al. 2025), 'Endosymbiotic Snowball Effect' was articulated (Wang et al. 2025). To test 'Endosymbiotic Snowball Effect', we further partitioned the genetic distance into mtDNA and nDNA distance to understand their independent and interactive effects on speciation. Together, this study will inform the mode of speciation in the origin of animal biodiversity.

Method

Hybrid zones

We built a database, "Hybrid Zone Explorer", including 315 animal hybrid zones reported to date and categorized them into six taxonomic groups: amphibians, birds, fishes, invertebrates, reptiles, and mammals (Fig. 2B). We synthesized existing reports hybrid zones (Gourbiere and Mallet 2010; McEntee et al. 2020; Nieto Feliner et al. 2023) and independently extracted cline variables from the primary literature for this study. To account for heterogeneity of cline widths, we recorded uncertainty estimates of the cline widths for each hybrid zone. We filtered the 315 animal hybrid zones with the following criteria: (1) there has been sufficient spatial sampling to fit the genetic and/or phenotypic clines across the hybrid zone; (2) there have been direct

159 estimations of cline widths with genetic markers; (3) there is sufficient information on dispersal
160 distance in the unit of Kilometer/generation or Kilometer/generation$^{0.5}$; (4) for the dispersal
161 distance reported in Kilometer/generation, there is information on generation time to convert to
162 the Kilometer/generation$^{0.5}$ for calculation of selection (see *Selection against hybrids* section
163 below) in the tension zone model (Barton and Gale 1993). These criteria resulted in 152
164 animal hybrid zones for model testing (see below).
165 *Mitonuclear genetic distance*
166 To infer the genetic distance between hybridizing species, we calculated the genetic
167 distance of the most sequenced mitochondrial and nuclear genes in animals. We surveyed a
168 broad panel of markers, including mitochondrial genes (Cytb, ND2, COI, ND3, ND4, Msh1),
169 nuclear protein-coding genes (RAG1, RAG2, MC1R, BDNF, ODC1, MHCII, ASIP, ACTB,
170 IRBP, ENC1, TYR, EF1A, GAPDH, Wnt1, H3, H4, FGB), cytoribosomal genes (5S, 18S, 28S,
171 ITS1, ITS2) and mitoribosomal genes (12S, 16S). We fetched DNA sequences of the target
172 genes for each parental species from GenBank and only kept the genes if both species had at
173 least three sequences per species. To ensure even sampling depths among the species pairs
174 in our meta-analysis, for species with more than 15 sequence records of a gene, we randomly
175 sampled 15 sequences among all the records. We then aligned all the sequences of each
176 gene in each species pair with the msa function in the msa package (Bodenhofer et al. 2015)
177 in R (R Core Team 2023). Specifically, we used MUSCLE (Edgar 2004) with gapOpening = 20
178 and gapExtension = 10. With the alignment, we calculated the mean pairwise distance
179 between parental species with dist.dna function with the TN93 substitution rate model in the
180 ape package (Paradis and Schliep 2019). Then, we averaged the between-species distance of

all the mitochondrial genes and nuclear genes separately to result in the mean pairwise mtDNA distance ($\overline{K_m}$) and the mean pairwise nDNA distance ($\overline{K_n}$) between each pair of parental species. Finally, we calculated the mean pairwise genetic distance ($\overline{K}$) between each pair of parental species by averaging the nDNA and mtDNA distances. To account for the uncertainty in $\overline{K}$ estimations, we calculated the standard deviation of $\overline{K_m}$, $\overline{K_n}$, and $\overline{K}$. Among the 152 hybrid zones, 99 hybrid zones had sufficient genetic information to calculate the genetic distance between parental species. To evaluate the reliability of our genic estimation of parental species divergence, we computed the ratio of between-species distance over the sum of between- and within-species distance and conducted correlation tests of F_{ST} estimates for several pairs of species reported in the literature (see supplementary data).

Selection against hybrids

We extracted the dispersal, center, and width of hybrid zones from McEntee et al. (2020), Nieto Feliner et al. (2023), and additional literature (supplementary data). We unified the unit of dispersal rate as kilometers (KM) /$\sqrt{generation}$ with the average generation time information of each species pair. To account for sex-specific dispersal, we conducted another round of literature search for female vs male dispersal rate in each species pair (supplementary information). We calculated the average cline width (w) and center for mtDNA and nDNA data, as well as phenotypic data separately. We calculated selection (s) against heterozygotes as a function of cline width (w) and dispersal (σ): $s = (2 \times \frac{\sigma}{w})^2$ (Fig. 1) (Barton and Gale 1993). To infer the cumulative selection against hybrids, we substituted w with averaged cline width ($\overline{w}$) among mtDNA and nDNA clines (Fig. 3B). To account for uncertainty of selection estimates due to heterogeneous dispersal rates and cline width estimates, we

monitored sex-specific dispersal, and the variance of cline width estimates for each hybrid zone. For hybrid zones with known sex-specific dispersal rates, we calculated selection on mtDNA and nDNA, respectively, as $s_{mt} = (2 \times \frac{\sigma(female)}{w})^2$ and $s_{mt} = (2 \times \frac{\sigma(average)}{w})^2$. We derived the standard deviation of selection (s), $SD(s) = (8\sigma^2 / w^3)\ SD(w)$. This composite standard deviation of selection (SD(s)) accounts for uncertainties of cline width estimation and heterogeneity of dispersal rates. Then we generate 95% CI with SD(s) to incorporate the composite uncertainty in the estimation of selection for each hybrid zone in the speciation models (see below).

Speciation models

To investigate the relationship between genetic distance and strength of selection against hybrids (s) in the hybrid zones, we test three conventional hybrid incompatibility models: (1) Linear Effect (Eq. 1.1), (2) Snowball Effect (Eq. 2.1; Fig. S1), and (3) Slowdown Effect (Eq. 3.1). In each model, selection (s) is a function of genetic distance (K) with a rate parameter r and a constant parameter C as divergent plasticity, epigenetic divergence, or epigenetic assimilation (Pigliucci and Murren 2003; Ehrenreich and Pfennig 2016; Mueller et al. 2025). The rate parameter corresponds to the average effect size of each pair of incompatibilities.

$$s = rK + C \qquad \text{(Eq. 1.1)}$$

$$s = 1 - e^{-(rK^2 + C)} \qquad \text{(Eq. 2.1)}$$

$$s = ln(rK + C) \qquad \text{(Eq. 3.1)}$$

To account for the effects of mtDNA and nuclear genetic distance between the parental species (Fig. 3), we further refined the conventional expressions (Eq. 1.1, 2.1, and 3.1) into

mitonuclear models (Eq. 1.2, 2.2, and 3.2) to partition K into K_m (mtDNA distance) and K_n (nuclear DNA distance) that correspond to rate parameters r_m and r_n, respectively, besides mitonuclear interaction r_{mn}, and a epigenomic constant of C.

$$s = r_m K_m + r_n K_n + r_{mn} K_m K_n + C \quad \text{(Eq. 1.2)}$$

$$s = 1 - e^{-(r_m {K_m}^2 + r_n {K_n}^2 + r_{mn} K_m K_n + C)} \quad \text{(Eq. 2.2)}$$

$$s = ln(r_m K_m + r_n K_n + r_{mn} K_m K_n + C) \quad \text{(Eq. 3.2)}$$

We conducted model fitting of the above three models with the nls2 function of nls2 package (Grothendieck, 2007) in R (R Core Team 2023). With the default algorithm and starting value of $r = 0.01$, $C = 0.1$, model fitting was conducted. The AIC of each fitted model is obtained with the AIC function. In each conventional model fitting (Eq. 1.1, 2.1, 3.1), we estimated the rate parameter r and constant C with selection against hybrid incompatibility (s) in response to mean pairwise genetic distance ($\overline{K}$) between the parental species. To evaluate independent effects of mtDNA and nDNA distance, we tested Eq. 1.1, 2.1, and 3.1 with K being $\overline{K_m}$ and $\overline{K_n}$.

To evaluate taxon-specific patterns, we conducted conventional model fitting (1.1, 2.1, 3.1) within each taxonomic group (Amphibians, Birds, Invertebrates, Mammals, and Reptiles), except for Fishes, due to data insufficiency. Furthermore, we estimated r_m, r_n, and C in the refined model fitting (1.2, 2.2, 3.2). Only 38 hybrid zones had sufficient mtDNA and nDNA sequence data to participate in refined model fitting, thus further taxon-specific modeling fitting was omitted.

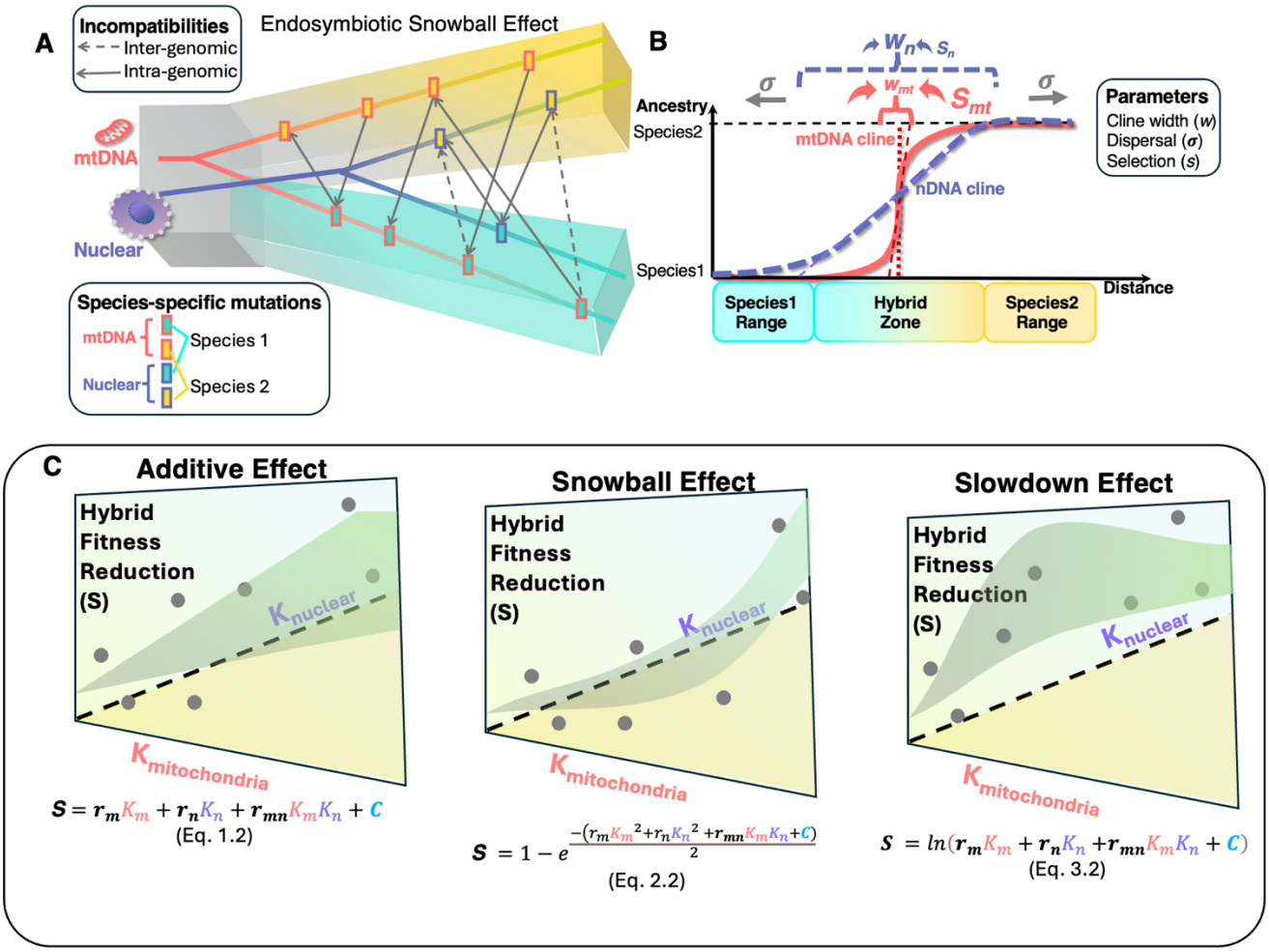


Fig. 3 Mitonuclear genetic divergence underlying the selection against hybrids. A. Endosymbiotic Snowball Effect (Wang et al. 2025): Lineage-specific substitutions in the mitochondrial genome (red) and nuclear genome (purple) can lead to intragenomic and intergenomic Dobzhansky-Muller Incompatibilities, which emergently contribute to selection against hybrids. **B.** This selection counteracts gene flow (σ) across hybrid zones and reduces the cline width (w). Greater substitution rates in the mitochondrial genome than the nuclear genome can result in a greater rate of incompatibility and thus stronger selection on mtDNA clines than the nDNA clines. **C**, Refined speciation models with independent and interactive mitonuclear effects: (1) Linear (Eq. 1.2), Snowball (Eq. 2.2), Slowdown (Eq. 3.2).

To test the significance of observed regression coefficients, we conducted 1,000 bootstrap iterations to generate a bootstrap distribution of regression coefficients $\hat{r}$ and $\hat{C}$. In each bootstrap iteration, we randomly sampled N = 152 hybrid zones with replacement from the full dataset. For each hybrid zone, we sampled *s* from the composite 95% CI

simultaneously accounting for heterogeneity of cline width and dispersal estimations. For each bootstrap sample of $K^* = [K_1^*, K_2^*, \ldots K_i^*, \ldots K_{152}^*]$ and $s^* = [s_1^*, s_2^*, \ldots s_i^*, \ldots s_{152}^*]$, we simultaneously fitted the sample to (1) Linear, (2) Snowball, and (3) Slowdown Effect Models (Fig.1; Eq. 1.1, 2.1, & 3.1) to calculate $\hat{r}$ and $\hat{C}$. To account for the uncertainty in K and s, we randomly sampled K_i^* and s_i^* respectively from normal distributions: $N(K_i, sd(K_i))$ *and* $N(s_i, sd(s_i))$. To generate a null distribution of $\hat{r}$ and $\hat{C}$, we randomly shuffled and mismatched K^* and s^* in each bootstrap sample and simultaneously fitted the three models (Eq. 1.1, 2.1, & 3.1) again. We used paired-T tests to compare the observed distribution of r and C, *r_Obs* and *C_Obs, to* the corresponding null distributions, *r_H0* and *C_H0*.

A similar bootstrapping test was applied to the refined models (Fig. 3C; Eq. 1.2, 2.2, & 3.2), where (1) Linear, (2) Snowball, (3) Slowdown Models were compared in terms of AICs, and the observed bootstrap distribution of $\widehat{r_m}$, $\widehat{r_n}$, $\widehat{r_{mn}}$, and $\hat{C}$, r_m*_Obs*, r_n*_Obs,* r_{mn}*_Obs* and *C_Obs*, was respectively compared to r_m*_H0*, r_n*_H0*, r_{mn}*_H0*, and *C_H0*.

Results

Discordant mitonuclear selection

The mtDNA and nDNA cline widths are significantly correlated ($R^2 = 0.44$, $p < 10^{-7}$). However, the selections against hybrids on mtDNA and nDNA are not significantly correlated ($R^2 = 0.02$, $p > 0.05$). The discrepancy of selection on mtDNA and nDNA clines significantly decreases with greater genetic distance between the parental species ($R^2 = 0.14$, $p = 0.03$).

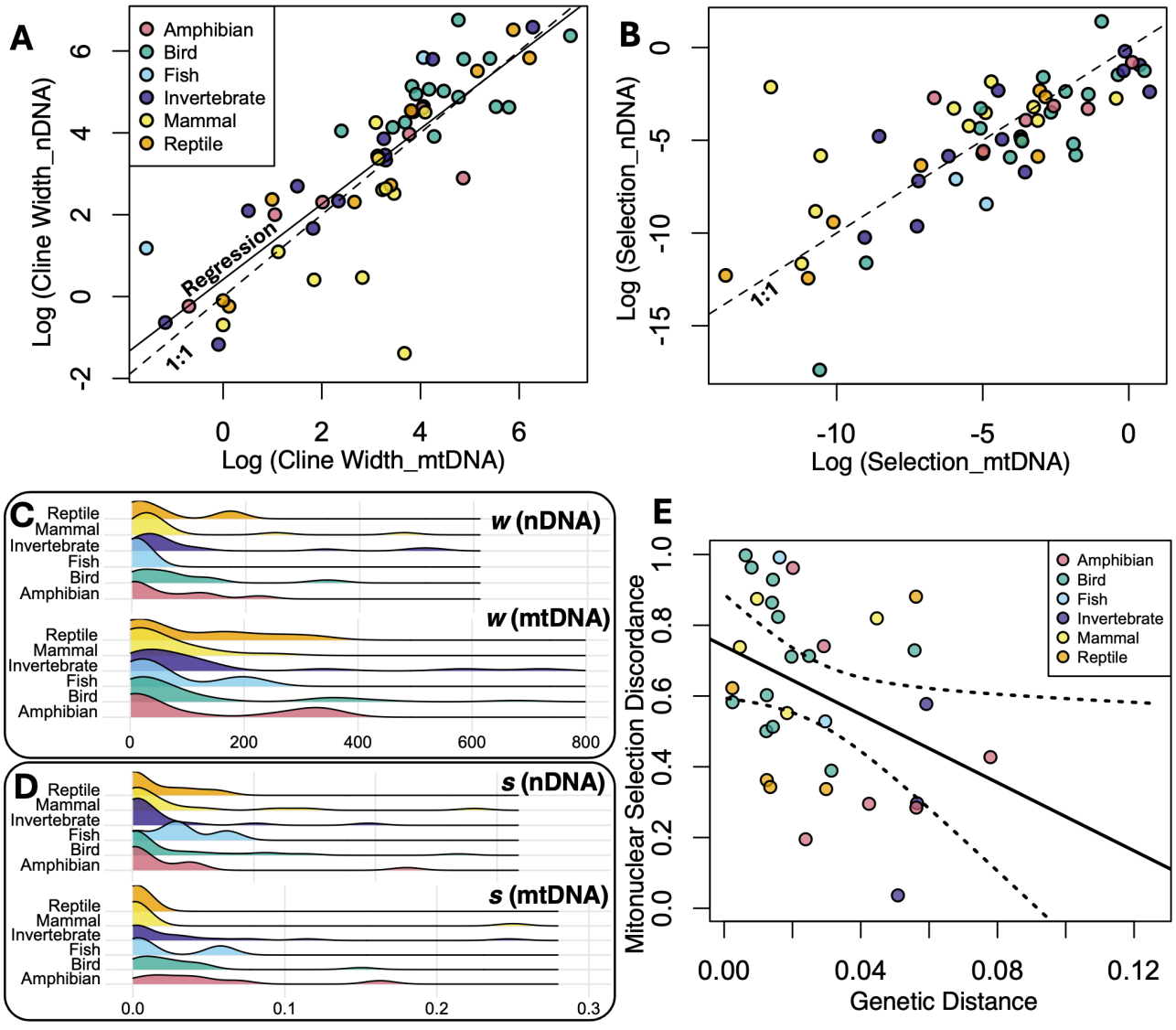


Fig. 4 Mitonuclear selection in animal hybrid zones. A, the cline widths (in KM) of mitochondrial and nuclear DNA in log scale were significantly correlated. The two variables are

significantly correlated ($r = 0.44$, $p < 10^{-7}$). **B**, Selection on mitochondrial clines and nuclear DNA clines were presented in log scales. **C-D**, The distribution of nuclear (nDNA) and mitochondrial (mtDNA) genetic cline widths (**C**) and selection on the clines (**D**) across animal taxa. **E**, the discordance between selections on mtDNA and nDNA significantly decreases with genetic distance ($p < 0.05$).

Speciation models

The Snowball Effect Model (3.2) (Fig. 1, 5A) has the lowest AIC when fitted to the full data, but it is only marginally superior with ΔAIC being 0.36. However, the Snowball Effect Model showed stronger superiority within amphibians (ΔAIC = 1.15), mammals (ΔAIC = 3.46), and reptiles (ΔAIC = 2) than the alternative model with the second lowest AIC (Table 1). However, the three models were about equal (ΔAIC = 0.05) for birds with the Beanbag Effect Model retaining the lowest AIC. When evaluating the effect of mitochondrial and nuclear genomic divergence separately, the Snowball Effect was strongly supported (ΔAIC = 4.21) for the nuclear genomic divergence (Table S1), but not mitochondrial genomic divergence (Table S2).

The bootstrap mean of *r_Obs* in the Snowball Effect model (Eq. 3.2) was 7.38 (Fig. 5B), which was significantly different from *r_H0* (mean difference: 4.79, 95% CI of the difference: 0.69 to 10.58, $p < 10^{-15}$), indicating a significantly positive effect of genetic divergence on selection against hybrids. However, the estimates of *r* were heterogeneous among taxonomic groups (Table 1), with birds ($r = 15.39$) being the highest, then mammals ($r = 10.84$), amphibians ($r = 8.89$) and invertebrates ($r = 8.69$) intermediate, and lower for reptiles ($r = 0.74$) (Table 1).

Table 1 The effect of genetic divergence on the selection against hybrids among animal taxa. Standard errors (SE) of the regression coefficients for the rate parameter(*r*) and constant (*C*). The models (Fig. 1, Eq 1.1-3.1) with the lowest AICs are in bold. The Snowball model (equation 3.1) has the lowest AIC fitted to the full dataset. The estimates of rate parameter(*r*) are not directly comparable among models.

Taxa	Models	*r*	SE (*r*)	*C*	SE (*C*)	AIC	ΔAIC
Altogether	Beanbag	6.452	1.995	-0.006	0.062	40.063	
	Snowball	11.376	2.021	0.051	0.054	**39.706**	0.36
	Slowdown	7.699	2.585	0.985	0.068	40.330	
Amphibian	Beanbag	5.497	2.998	-0.114	0.140	0.655	
	Snowball	8.890	2.317	-0.047	0.098	**-0.500**	**1.16**
	Slowdown	5.636	3.485	0.895	0.145	1.036	
Bird	Beanbag	10.002	4.828	-0.024	0.149	**27.597**	
	Snowball	15.394	4.828	0.058	0.134	27.649	0.05
	Slowdown	12.972	6.935	0.953	0.167	27.705	
Invertebrate	Beanbag	5.271	2.112	-0.024	0.097	3.660	
	Snowball	8.685	2.066	0.022	0.087	**3.265**	0.40
	Slowdown	6.343	2.892	0.970	0.103	3.915	
Mammal	Beanbag	6.060	2.224	-0.113	0.078	-11.164	
	Snowball	10.842	1.667	-0.062	0.050	**-14.625**	**3.46**
	Slowdown	5.957	2.462	0.898	0.080	-10.417	
Reptile	Beanbag	0.047	0.028	0.001	0.001	-60.764	
	Snowball	0.739	0.158	0.001	0.001	**-62.765**	**2.01**
	Slowdown	0.047	0.028	1.001	0.001	-60.760	

When considering mitonuclear genetic divergence independently and interactively (Fig. 3), the Snowball Effect model (Eq. 2.2) has the lowest AIC (Table 2; Fig. 5 C-D). Remarkably, the ΔAIC between the Snowball Effect model and the next model was 8.8. We observed a significantly positive effect of nuclear DNA distance and mDNA distance independently, but a negative interactive effect of mitonuclear genetic distance (Fig. 5C) on the selection against hybrid DNA. Specifically, the nuclear genetic divergence effect (r_n) was large (Table 2). In the Snowball Effect Model, bootstrap mean of r_n was significantly different from r_n*_H0* (mean

322 difference: 667.01, 95%CI of the difference: 620.15 to 713.87 $p < 10^{-15}$) (Fig. 5D). In
323 comparison, the estimated mitochondrial genetic divergence effect (r_m) was much smaller
324 (Table 2) but was significantly different than r_{m_H0} (mean difference: 77.12, 95%CI of the
325 difference: 71.75 to 82.49; $p < 10^{-15}$). The regression coefficient of mitonuclear interactive
326 effect (r_{mn}) was significantly negative, with the bootstrap mean significantly more negative than
327 r_{mn_H0} (mean difference: -635.573, 95%CI of the difference: -671.84 to -599.31; $p < 10^{-15}$).
328
329 **Table 2** Regression coefficients and standard errors (SE) of the r_m, r_n, and C of the refined
330 models. The Snowball Effect model has the lowest AIC.

Models	r_m	**SE (** r_m **)**	r_n	**SE (** r_n **)**	r_{mn}	**SE (** r_{mn} **)**	C	**SE (** C **)**	**AIC**
Beanbag	6.10	2.15	19.65	4.718	-400.28	107.44	-0.09	0.08	8.18
Snowball	**189.59**	**73.72**	**1214.69**	**610.01**	**-1096.37**	**439.58**	**0.14**	**0.107**	**-0.63**
Slowdown	6.38	2.73	21.01	7.819	-417.79	139.83	0.92	0.10	11.82

331

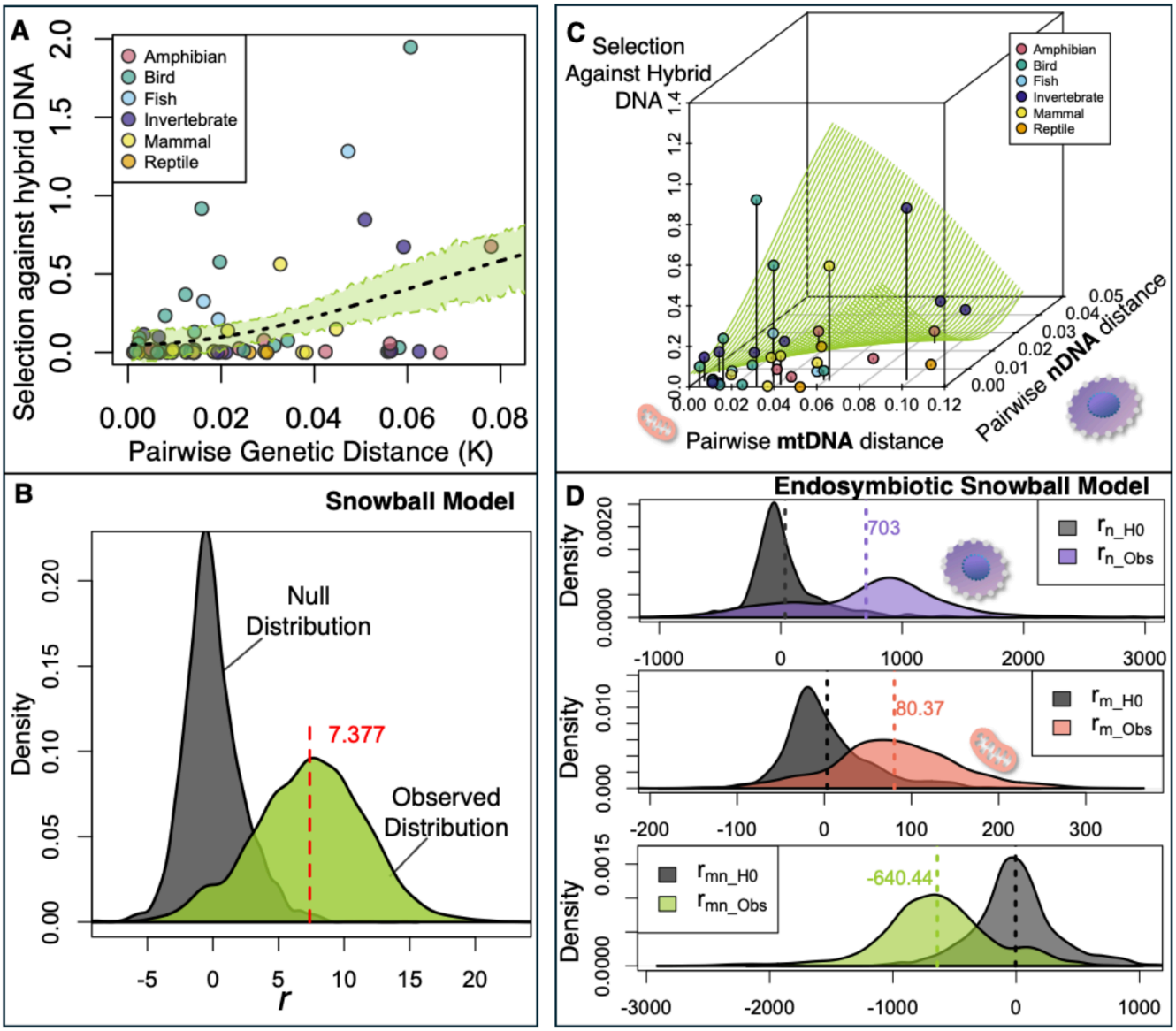


Fig. 5 Coefficients of estimates in the best-fitted models for conventional versus refined models of speciation. A, Conventional models (equations 1.1, 2.1, and 3.1) considered the total genetic distance as the predictor for selection against hybrids. The Snowball Effect model (dotted line) has the lowest AIC. **B**, Bootstrap distributions of the rate parameter *r* (equation 1.3) estimations based observed relationship between *K* and *s* across animal hybrid zones (blue) versus *r* estimates based on randomly mismatched *K* and *s* (grey). Estimates of *r* are based on the best-fitted conventional models. **C**, Refined models considered the effect of mtDNA and nDNA divergence and their interactions separately. The Snowball Effect model again has the lowest AIC. **D**, The bootstrap distributions of rate parameter estimations for r_m, r_n, and r_{mn} which correspond to the independent effects of mtDNA and nDNA distance as well as their interaction. Estimates of r_m, r_n, and r_{mn} are from the best-fitted refined model. **C**-**D**, vertical dotted lines represent bootstrap means.

Discussion

The accumulation of selection against hybrids in the hybrid zones between diverging lineages is key to unraveling speciation rates *in situ*. Here, we leveraged decades of hybrid zone studies to understand the evolution of reproductive isolation in the face of gene flow. Overall, the selection against hybrids increased with genetic divergence between the parental species, despite the heterogeneous speciation rates across taxa (Table 1, 2; Fig. 5).

The Snowball Effect Models (Equation 2.1 & 2.2) best fitted the full data (Fig. 5, Table 1-2) among the conventional models (Equation 1.1-3.1, Fig. 1) as well as the refined models (equation 1.2-3.2, Fig. 3). The taxon-specific results are largely concordant with the full data supporting the Snowball Effect. Altogether, our results suggest that Dobzhansky & Muller Incompatibilities (DMIs) (Dobzhansky 1934; Muller 1942; Mayr 1963) predominately contribute to barriers to gene flow. This conclusion is consistent with previous empirical studies on fruit flies and wild tomato (Presgraves 2002; Matute et al. 2010; Moyle and Nakazato 2010). Despite the challenge to maintain epistatic co-adaptive variants during speciation with gene flow (Felsenstein, 1981), epistasis can snowball barriers to gene flow across the genomes, allowing speciation to rapidly proceed (Orr, 1995).

Specifically, estimate of rate parameter r was the highest in birds (Table 1) which reflects strong role of genetic divergence in speciation with gene flow. High basal metabolic rates in endotherms could require stronger selection on genetic incompatibility, especially between the mitochondrial and nuclear genomes (Hill 2019). As endotherms exhibit faster climatic niche shifts than ectotherms (Rolland et al. 2018), the underlying genetic divergence between endothermic sister populations could disproportionately contribute to divergent

367 adaptation. Both the proximate and ultimate differences in endotherms vs ectotherms could
368 lead to greater effect sizes of genetic divergence on the selection against hybrids.
369 The three speciation models (Fig. 1) are not necessarily mutually exclusive and could
370 be parallel, sequential, or hierarchical in the genome evolution underlying speciation. In the
371 early stage of speciation, the growth of reproductive isolation via a single or few large-effect
372 substitutions (Nosil and Schluter 2011; Servedio et al. 2011), genetic assimilation (Waddington
373 1961), and/or cultural evolution (Lachlan and Servedio 2004) prior to extensive genetic
374 divergence renders a Slowdown Effect (Gourbiere and Mallet 2010). Independent
375 genetic/epigenetic effects could rapidly and synergistically couple with other locally adaptive
376 loci to form DMIs (Dobzhansky 1934; Muller 1942; Mayr 1963) and/or genome-wide barriers to
377 gene flow (Flaxman et al. 2013).
378 The initial independent reproductive isolation might experience organismal constraints
379 and thus are heterogeneous among taxonomic groups. For example, vocal learning in
380 songbirds might uniquely increase the likelihood of cultural evolution as premating isolation
381 (Slabbekoorn and Smith 2002; Lachlan and Servedio 2004), though it can also disrupt
382 reproductive isolation. Future combinatorial examination of the three models in different parts
383 of the nuclear genome could further unveil the evolutionary genomic mechanism of speciation.
384 When we consider the mtDNA and nDNA divergence separately (Eq. 1.2, 2.2, 3.2),
385 Snowball Effect model (Eq. 2.2) fits the data best (Fig. 1). In this model, nuclear and
386 mitochondrial divergence showed large positive effects, while the mitonuclear interaction
387 exhibited negative effects (Fig. 5C, Table 2). This result is concordant with the conventional
388 model (Fig. 5A) in terms of the overall positive role of mtDNA or nDNA divergence on barriers

to gene flow. The interaction of mtDNA and nDNA distance showed a negative role for barriers to gene flow (Fig. 5C). This pattern may seem inconsistent with the growing evidence that mitonuclear incompatibility being important for early-stage speciation (Hill 2017; Wang et al. 2021; Burton 2022; Moran et al. 2024). Greater mutation rates of mtDNA than nDNA in animal cells (Ballard and Whitlock 2003; Lynch et al. 2006) were expected to result in mitonuclear ancestry discordance. While some of the mitonuclear ancestry discordance may contribute to interspecific incompatibility (Orr 1995), some could be beneficial (Havird et al. 2019; Garde et al. 2025).

We observed much smaller effect sizes of independent mitochondrial substitutions on hybrid fitness (Fig. 5, r_m), which could be a result of strong mitochondrial purifying selection and nuclear compensatory evolution. The roughly 5-fold greater effect sizes of mitochondrial deleterious mutations than nuclear mutations (Popadin et al. 2013) incurs greater purifying selection (Popadin et al. 2013) in the mitochondrial genome. Further compensatory evolution of the nuclear genome (Princepe and De Aguiar 2024) could mask the initial independent effects of mitochondrial substitutions. Indeed, we observed the narrower mtDNA cline than the nDNA cline (Fig. 4) despite the smaller effective population size of mtDNA than nDNA expected greater drift and a wider cline under neutrality (Slatkin and Maruyama 1975).

Caveats

The available 315 animal hybrid zone studies have been concentrated in the global northwest (Fig. 2B, S2), with an underrepresentation of global biodiverse hotspots. Our observation could be predominantly representing animal speciation patterns in western temperate ecoregions (Weir & Schluter, 2007), which may not apply for tropical ecoregions as

411 eco-evolutionary dynamics can be intricate and complex in highly biodiverse ecosystems
412 (Burney & Brumfield, 2009). There are far fewer aquatic hybrid zones than terrestrial hybrid
413 zones (Fig. 2B), which may constrain our conclusion within the terrestrial domain. Life history
414 information, such as independently measured generation time and dispersal rate, was
415 unavailable for a large proportion of the hybrid zones, with only 152 of the 315 cases
416 containing sufficient information to calculate selection against hybrids. For the 152 hybrid
417 zones for which we could calculate selection, there were insufficient sequence data in
418 GenBank for commonly sequenced genes in the nuclear genomes of the species pairs. This
419 sequencing gap limits the inference from the refined models to a small sample size. Despite
420 the limited dataset, the significant mitonuclear effect on the selection against hybrid DNAs
421 supported the Endosymbiotic Snowball Effect (Wang et al. 2025). Future studies that broaden
422 the sequencing scope of hybrid zone studies could provide valuable modeling resolution to
423 illuminate speciation heterogeneity across the genomes.
424 The our metrics of selection against hybrids leveraged tension zone model (Barton and
425 Gale 1993) assuming the balance of selection and dispersal, which may not be generally
426 applicable. However, even without reaching selection and dispersal balance, the ratio of cline
427 width and dispersal rate still reflects the extent of barriers to gene flow across the nascent
428 species boundaries of naturally hybridizing taxa and thus remains the most direct population
429 metrics of speciation in situ. Since the understanding of organismal gene flow is crucial for
430 biodiversity science and conservation in the increasingly fragmented biosphere (Wang and
431 Yoder 2025), further developing direct and standardized metrics to monitor gene flow across
432 the species boundaries can be productive for speciation and conservation science.

Conclusion

We investigated the evolutionary trajectories of barriers to gene flow in the early stage of speciation, empowered by decades of animal hybrid zone studies. The data supported the exponential growth of selection against hybrid DNA with increased mitonuclear genetic divergence, consistent with the Endosymbiotic Snowball Effect (Wang et al. 2025). Future broadening of taxonomic breath and dissection of the regularity and specificity of barriers to gene flow would be indispensable for refining our understanding of speciation rates across the tree of life.

Reference

Ballard WO, Whitlock MC (2004) The incomplete natural history of mitochondria. *Mol Ecol* 13:729–744.

Barton NH (1979) The dynamics of hybrid zones. *Heredity* 43:341–359.

Barton NH, Gale KS (1993) Genetic analysis of hybrid zones. In: *Hybrid Zones and the Evolutionary Process*, pp. 13–45. Oxford University Press, Oxford, UK.

Barton NH, Hewitt GM (1985) Analysis of hybrid zones. *Annu Rev Ecol Syst* 16:113–148.

Bodenhofer U, Bonatesta E, Horejš-Kainrath C, Hochreiter S (2015) msa: An R package for multiple sequence alignment. *Bioinformatics* 31:3997–3999.

Burney CW, Brumfield RT (2009) Ecology predicts levels of genetic differentiation in Neotropical birds. *Am Nat* 174:358–368.

Burton RS (2022) The role of mitonuclear incompatibilities in allopatric speciation. *Cell Mol Life Sci* 79:103.

Coyne JA, Orr HA (1989) Patterns of speciation in *Drosophila*. *Evolution* 43:362–381.

de Zwaan DR, Mackenzie J, Mikkelsen E, Wood C, Wang S (2022) Pleiotropic opposing dominance within a color gene block contributes to a nascent species boundary via its influence on hybrid male territorial behavior. *PNAS Nexus* 1:pgac074.

Dobzhansky T (1934) Studies on hybrid sterility. *Z Zellforsch Mikrosk Anat* 21:169–223.

Eddo D, Hodur Z, Wang S (2025) The hidden figures at species boundaries: The mitochondrial energetics behind mating signal divergence. *Integr Comp Biol*. icaf058.

Edgar RC (2004) MUSCLE: Multiple sequence alignment with high accuracy and high throughput. *Nucleic Acids Res* 32:1792–1797.

Ehrenreich IM, Pfennig DW (2016) Genetic assimilation: A review of its potential proximate causes and evolutionary consequences. *Ann Bot* 117:769–779.

Feder JL, Nosil P, Wacholder AC, Egan SP, Berlocher SH, Flaxman SM (2014) Genome-wide congealing and rapid transitions across the speciation continuum during speciation with gene flow. *J Hered* 105:810–820.

Felsenstein J (1981) Skepticism towards Santa Rosalia, or why are there so few kinds of animals? *Evolution* 35:124.

Fisher RA (1930) *The Genetical Theory of Natural Selection*. pp 36-41. Clarendon Press, Oxford, UK.

Fisher RA (1941) Average excess and average effect of a gene substitution. *Ann Eugen* 11:53–63.

Flaxman SM, Feder JL, Nosil P (2013) Genetic hitchhiking and the dynamic buildup of genomic divergence during speciation with gene flow. *Evolution* 67:2577–2591.
Gavrilets S (2004) *Fitness Landscapes and the Origin of Species*. Princeton University Press, Princeton, NJ.
Gourbière S, Mallet J (2010) Are species real? The shape of the species boundary with exponential failure, reinforcement, and the "missing snowball." *Evolution* 64:1–24.
Grothendieck G (2007) *nls2: Non-Linear Regression with Brute Force*. R package.
Haldane JBS (1964) A defense of beanbag genetics. *Perspect Biol Med* 7:343–359.
Havird J, Forsythe E, Williams A, Werren JH, Dowling DK, Sloan D (2019) Selfish mitonuclear conflict. *Curr Biol* 29:R496–R511.
Hill GE (2017) The mitonuclear compatibility species concept. *Auk* 134:393–409.
Hill GE (2019) *Mitonuclear Ecology*. Oxford University Press, Oxford, UK.
Lachlan RF, Servedio MR (2004) Song learning accelerates allopatric speciation. *Evolution* 58:2049–2063.
Lijtmaer DA, Mahler B, Tubaro PL (2003) Hybridization and postzygotic isolation patterns in pigeons and doves. *Evolution* 57:1411–1418.
Lynch M, Koskella B, Schaack S (2006) Mutation pressure and the evolution of organelle genomic architecture. *Science* 311:1727–1730.
Matute DR, Butler IA, Turissini DA, Coyne JA (2010) A test of the snowball theory for the rate of evolution of hybrid incompatibilities. *Science* 329:1518–1521.
Mayr E (1959) Where are we? *Cold Spring Harb Symp Quant Biol* 24:1–14.
Mayr E (1963) *Animal Species and Evolution*. Harvard University Press, Cambridge, MA.
McEntee JP, Burleigh JG, Singhal S (2020) Dispersal predicts hybrid zone widths across animal diversity: Implications for species borders under incomplete reproductive isolation. *Am Nat* 196:9–28.
Moran BM, Payne CY, Powell DL, Iverson ENK, Donny AE, Banerjee SM, Langdon QK, Gunn TR, Rodriguez-Soto RA, Madero A, Baczenas JJ, Kleczko KM, Liu F, Matney R, Singhal K, Leib RD, Hernandez-Perez O, Corbett-Detig R, Frydman J, Gifford C, Schartl M, Havird JC, Schumer M (2024) A lethal mitonuclear incompatibility in complex I of natural hybrids. *Nature* 626:119–127.
Moyle LC, Nakazato T (2010) Hybrid incompatibility "snowballs" between *Solanum* species. *Science* 329:1521–1523.
Mueller SA, Merondun J, Lečić S, Wolf JBW (2025) Epigenetic variation in light of population genetic practice. *Nat Commun* 16:1028.
Muller HJ (1942) Isolating mechanisms, evolution, and temperature. *Biol Symp* 6:71–125.
Nieto Feliner G, Criado Ruiz D, Álvarez I, Villa-Machío I (2023) The puzzle of plant hybridisation: A high propensity to hybridise but few hybrid zones reported. *Heredity* 131:307–315.
Nosil P (2008) Speciation with gene flow could be common. *Mol Ecol* 17:2103–2106.
Nosil P, Schluter D (2011) The genes underlying the process of speciation. *Trends Ecol Evol* 26:160–167.
Orr HA (1995) The population genetics of speciation: The evolution of hybrid incompatibilities. *Genetics* 139:1805–1813.
Palopoli M, Wu CI (1994) Genetics of hybrid male sterility between *Drosophila* sibling species: A complex web of epistasis is revealed in interspecific studies. *Genetics* 138:329–341.
Paradis E, Schliep K (2019) ape 5.0: An environment for modern phylogenetics and evolutionary analyses in R. *Bioinformatics* 35:526–528.
Pigliucci M, Murren CJ (2003) Perspective: Genetic assimilation and a possible evolutionary paradox: Can macroevolution sometimes be so fast as to pass us by? *Evolution* 57:1455–1464.
Popadin KY, Nikolaev SI, Junier T, Baranova M, Antonarakis SE (2013) Purifying selection in mammalian mitochondrial protein-coding genes is highly effective and congruent with evolution of nuclear genes. *Mol Biol Evol* 30:347–355.

Presgraves DC (2002) Patterns of postzygotic isolation in Lepidoptera. *Evolution* 56:1168–1183.
Princepe D, de Aguiar MAM (2024) Nuclear compensatory evolution driven by mito-nuclear incompatibilities. *Proc Natl Acad Sci USA* 121:e2411672121.
R Core Team (2023) *R: A Language and Environment for Statistical Computing*. R Foundation for Statistical Computing, Vienna, Austria.
Rolland J, Silvestro D, Schluter D, Guisan A, Broennimann O, Salamin N (2018) The impact of endothermy on the climatic niche evolution and the distribution of vertebrate diversity. *Nat Ecol Evol* 2:459–464.
Roux C, Fraïsse C, Romiguier J, Anciaux Y, Galtier N, Bierne N (2016) Shedding light on the grey zone of speciation along a continuum of genomic divergence. *PLoS Biol* 14:e2000234.
Seehausen O, Butlin RK, Keller I, Wagner CE, Boughman JW, Hohenlohe PA, Peichel CL, Saetre GP, Bank C, Brännström Å, Brelsford A, Clarkson CS, Eroukhmanoff F, Feder JL, Fischer MC, Foote AD, Franchini P, Jiggins CD, Jones FC, Lindholm AK, Lucek K, Maan ME, Marques DA, Martin SH, Matthews B, Meier JI, Möst M, Nachman MW, Nonaka E, Rennison DJ, Schwarzer J, Watson ET, Westram AM, Widmer A (2014) Genomics and the origin of species. *Nat Rev Genet* 15:176–192.
Servedio MR, van Doorn GSV, Kopp M, Frame AM, Nosil P (2011) Magic traits in speciation: "Magic" but not rare? *Trends Ecol Evol* 26:389–397.
Slabbekoorn H, Smith TB (2002) Bird song, ecology and speciation. *Philos Trans R Soc Lond B Biol Sci* 357:493–503.
Slatkin M, Maruyama T (1975) Genetic drift in a cline. *Genetics* 81:209–222.
Stelkens RB, Young KA, Seehausen O (2010) The accumulation of reproductive incompatibilities in African cichlid fish. *Evolution* 64:617–633.
Waddington CH (1961) Genetic assimilation. In: *Advances in Genetics*, pp. 257–293. Elsevier.
Wang S, Mank JE, Ortiz-Barrientos D, Rieseberg LH (2025) Genome architecture and speciation in plants and animals. *Mol Ecol*. e70004.
Wang S, Ore MJ, Mikkelsen EK, Lee-Yaw J, Toews DPL, Rohwer S, Irwin D (2021) Signatures of mitonuclear coevolution in a warbler species complex. *Nat Commun* 12:4279.
Wang S, Rohwer S, de Zwaan DR, Toews DPL, Lovette IJ, Mackenzie J, Irwin D (2020) Selection on a small genomic region underpins differentiation in multiple color traits between two warbler species. *Evol Lett* 4:502–515.
Wang S, Yoder AD (2025) Synergies between speciation and conservation science yield novel insights for mitigating the biodiversity crisis of the Anthropocene. *Proc Natl Acad Sci USA* 122:e2500713122.
Weir JT, Schluter D (2007) The latitudinal gradient in recent speciation and extinction rates of birds and mammals. *Science* 315:1574–1576.
Welch JJ (2004) Accumulating Dobzhansky–Muller incompatibilities: Reconciling theory and data. *Evolution* 58:1145–1156.
Westram AM, Stankowski S, Surendranadh P, Barton N (2022) What is reproductive isolation? *J Evol Biol* 35:1143–1164.
Wu C-I (2001) The genic view of the process of speciation. *J Evol Biol* 14:851–865.

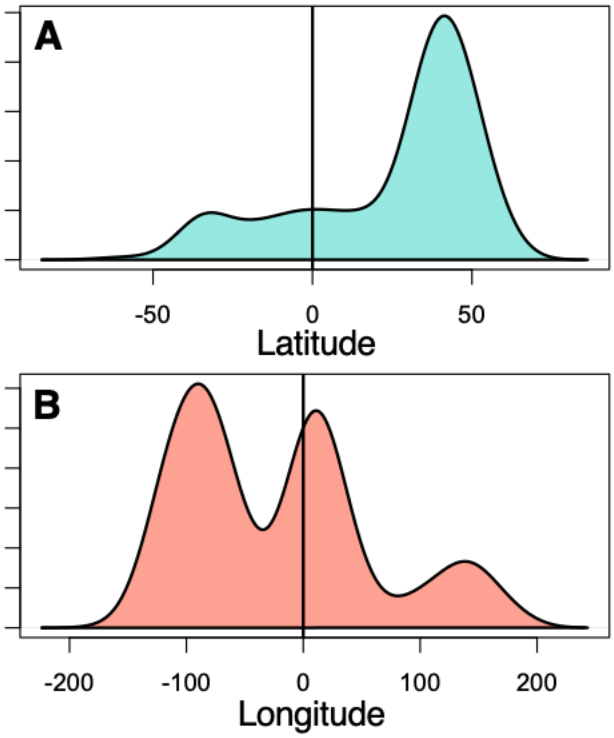
Data Accessibility

All the data involved in the analysis is available in Hybrid Zone Explorer database.

https://hzexplorer-production.up.railway.app/.

Supplement

Fig. S1. **Modified Snowball Effect**. Orr (1995) derived the cumulative effect of *K* substitutions with average effect size *r* on reduction of hybrid fitness, or the "strength of reproductive isolation" as $1 - e^{-rK^2/2}$ (see Eq. 8 in Orr 1995). To incorporate epigenetic effects and be directly comparable to Linear and Slowdown effects (Eq. 1.1 and 1.3), we modified the original form and examined its form with different *r* values at moderate *C*.



575
576 **Fig. S2. Density distribution of the latitude and longitude of known hybrid zones.** The
577 known hybrid zones have been concentrated on the northern (A) and western (B) hemisphere.

Table S1 The effect of nuclear genetic divergence on the selection against hybrids among animal taxa. Standard errors (SE) of the regression coefficients for the rate parameter(*r*) and constant (*C*). The models (Fig. 1, Eq 1.1-3.1) with the lowest AICs are in bold. The Snowball Effect Model (equation 3.1) has the lowest AIC fitted to the full dataset with strong superiority ($\Delta AIC > 4$) than the second model. ΔAICs (with >1 values bolded) represent the absolute difference in AIC between the models with the lowest and second lowest AIC for each taxonomic category.

Taxa	**Models**	***r***	**SE (*r*)**	***C***	**SE (*C*)**	**AIC**	**ΔAIC**
Altogether	Linear	5.568	3.050	0.085	0.057	16.771	**4.21**
	Snowball	12.754	3.867	0.109	0.053	**12.562**	
	Slowdown	5.497	4.154	1.100	0.066	17.521	
Amphibian	Linear	2.484	1.486	-0.004	0.025	-18.579	**1.59**
	Snowball	10.104	2.281	0.005	0.016	**-20.164**	
	Slowdown	2.533	1.538	0.996	0.026	-18.526	
Bird	Linear	-26.636	28.905	0.270	0.130	8.983	0.01
	Snowball	NA	NA	NA	NA	NA	
	Slowdown	-30.789	31.530	1.307	0.165	8.975	
Invertebrate	Linear	-4.519	5.268	0.179	0.118	5.750	0.02
	Snowball	NA	NA	NA	NA	NA	
	Slowdown	-4.777	5.512	1.192	0.137	5.768	
Mammal	Linear	-10.701	16.766	0.191	0.144	3.279	0.03
	Snowball	NA	NA	NA	NA	NA	
	Slowdown	-12.426	18.293	1.212	0.170	3.250	
Reptile	Linear	0.009	0.369	0.002	0.005	-19.659	0.00
	Snowball	NA	NA	NA	NA	NA	
	Slowdown	0.009	0.369	1.002	0.005	-19.659	

Table S2 The effect of mitochondrial genetic divergence on the selection against hybrids among animal taxa. Standard errors (SE) of the regression coefficients for the rate parameter(*r*) and constant (*C*). The models (Fig. 1, Eq 1.1-3.1) with the lowest AICs are in bold. The Slowdown Effect Model (equation 3.3) has the lowest AIC fitted to the full dataset. ΔAICs (with >1 values bolded) represent the absolute difference in AIC between the models with the lowest and second lowest AIC for each taxonomic category.

Taxa	**Models**	***r***	**SE (*r*)**	***C***	**SE (*C*)**	**AIC**	**ΔAIC**
Altogether	Linear	3.565	1.606	0.040	0.065	45.306	0.10
	Snowball	7.012	1.881	0.090	0.058	46.164	
	Slowdown	4.395	2.017	1.031	0.072	**45.202**	
Amphibian	Linear	3.102	3.133	-0.055	0.184	3.001	0.17
	Snowball	6.175	2.956	-0.012	0.140	**2.830**	
	Slowdown	3.294	3.389	0.944	0.187	3.040	
Bird	Linear	10.002	4.828	-0.024	0.149	**27.597**	0.05
	Snowball	15.394	4.828	0.058	0.134	27.649	
	Slowdown	12.972	6.935	0.953	0.167	27.705	
Invertebrate	Linear	5.271	2.112	-0.024	0.097	3.660	0.40
	Snowball	8.685	2.066	0.022	0.087	3.265	
	Slowdown	6.343	2.892	0.970	0.103	3.915	
Mammal	Linear	6.060	2.224	-0.113	0.078	-11.164	**3.46**
	Snowball	10.842	1.667	-0.062	0.050	**-14.625**	
	Slowdown	5.957	2.462	0.898	0.080	-10.417	
Reptile	Linear	0.047	0.028	0.001	0.001	-60.764	**2.00**
	Snowball	0.739	0.158	0.001	0.001	**-62.765**	
	Slowdown	0.047	0.028	1.001	0.001	-60.760	